



ISSN: 0067-2904

## Theoretical Study of Nuclear Density Distributions and Elastic Electron Scattering form Factors for Some Halo Nuclei

**Arkan R. Ridha\*, Mustafa K. Suhayeb**

Department of Physics, College of Science, University of Baghdad, Baghdad-Iraq

### Abstract

The nuclear matter density distributions, elastic electron scattering charge form factors and root-mean square (rms) proton, charge, neutron and matter radii are studied for neutron-rich  $^{6,8}\text{He}$  and  $^{19}\text{C}$  nuclei and proton-rich  $^8\text{B}$  and  $^{17}\text{Ne}$  nuclei. The local scale transformation (LST) are used to improve the performance radial wave function of harmonic-oscillator wave function in order to generate the long tail behavior appeared in matter density distribution at high  $r$ . A good agreement results are obtained for aforementioned quantities in the used model.

**Keywords:** halo nuclei, nuclear density distributions, elastic electron scattering form factors, root-mean square radii.

## دراسة نظرية لتوزيعات الكثافة النووية وعوامل التشكل للاستطارة الالكترونية المرنة لبعض النوى الهالة

**أركان رفعه رضا\* ، مصطفى خالد صحيب**

قسم الفيزياء، كلية العلوم، جامعة بغداد، بغداد، العراق.

### الخلاصة

تم دراسة توزيعات الكثافة الكتلية النووية بالإضافة الى عوامل التشكل الشحنة للاستطارة الالكترونية المرنة و انصاف الاقطان البروتونية والشحنة والنويوتونية والكتلية للنوى الغنية بالنيترونات،  $^{6,8}\text{He}$  و  $^{19}\text{C}$  بالإضافة الى النوى الغنية بالبروتونات،  $^8\text{B}$  و  $^{17}\text{Ne}$ . تم استخدام تحويل المقاييس الموضعى لتحسين اداء الدوال الموجية القطرية للمتنبب التواافقى لتوليد التنبيل الظاهر في توزيع الكثافة الكتلية عند الابعاد الكبيرة. تم استحصلان تطابق جيد جدا مع القيم العملية للكميات المذكورة اعلاه باستخدام هذا الانموذج.

### Introduction

In the mid-eighties, the pioneering discovery of steep rise of total interaction cross-section ( $\sigma_I$ ) by Tanihata and coworkers [1] induced by the scattering unstable nuclei on stable targets. Such large enhancement is mainly attributed to the large spatial extension in the matter density distribution explained by halo [2]. The nuclear halo in general are composed of loosely bound valence neutron(s) or proton(s) (the halo), surrounding a compact core. such large diffusivity causes unusual spatial properties of the nucleon density distribution, leading to nuclear sizes deviating substantially from the  $R \approx r_0 A^{1/3}$  rule.

\*Email: arkan\_rifaah@yahoo.com

The use of radial wavefunction of harmonic-oscillator (HO) potential to calculate density distributions in the no-core shell model for light nuclei resulted in poor agreement with experimental data [3-6]. Besides that, two frequency shell model (TFSM) approach was employed on halo nuclei [7-9] with variant success. Within this model, one can use two HO size parameters, one for bound core ( $b_{core}$ ) and second for loosely bound valence nucleon(s) ( $b_{halo}$ ), respectively. The transformed HO basis derived by local scale transformation is a promising approach to regenerate the long tail behavior in the density distribution [10,11]. knowing that the radial wavefunction of HO potential have Gaussian decay at large  $r$  on contrary to the observed behavior of density distribution which have exponentially decay. The proton and neutron density distributions are calculated with acceptable results using LST for  $^{6,8}\text{He}$  and  $^{11}\text{Li}$  but with overestimated rms radii [12]. The LST applied with a good success to calculate the scattering phase-shifts and the electric transition probabilities  $B(E1)$  and  $B(E2)$  for  $^6\text{He}$  scattered by  $^{12}\text{C}$  and  $^{208}\text{Pb}$  [13]. The nuclear Skyrme Hartree-Fock and Hartree-Fock Bogoliubov are solved using the cylindrical transformed deformed HO basis to calculate density distributions and axial multipole moments [14]. The cylindrical transformed deformed HO basis is applied successfully to solve the nuclear Hartree-Fock and Hartree-Fock Bogoliubov to find the nuclear collective inertia at the perturbative cranking approximation and fission fragments charge, mass and deformations [15].

This work is dedicated to calculate proton, charge, neutron and matter density distributions, the corresponding *rms* radii, and elastic electron charge form factors for exotic  $^{6,8}\text{He}$ ,  $^8\text{B}$ ,  $^{19}\text{C}$  and  $^{17}\text{Ne}$  nuclei.

### Theoretical basis

The nuclear density distributions of point neutron and proton for halo nuclei can be formulated as [16]:

$$\rho_{n/p}(r) = \rho_{n/p}^{core}(r) + \rho_{n/p}^{halo}(r) \quad (1)$$

where  $\rho_{n/p}^{core}(r)$  represents the neutron/proton density distributions of core part calculated using the radial wave functions ( $R_{nl}(r)$ ) of HO potential [17] as follows:

$$\rho_{n/p}^{core}(r) = \frac{1}{4\pi} \sum_{nl} X_{n/p}^{nl,core} |R_{nl}(r, b_{n/p})|^2 \quad (2)$$

where  $X_{n/p}^{nl,core}$  represents an integer number denoting the neutrons/protons occupation number in the  $nl$  shell;  $n$  and  $l$  represent the principal and orbital quantum numbers respectively.  $b_{n/p}$ , represents the HO size parameters for neutron/proton. The summation in Eq. (2) spans all occupied orbits of the core part of any nuclear sample under study. The matter density distribution for the core can be written as the sum of densities of core neutrons and protons ( $\rho_m^{core}(r) = \rho_p^{core}(r) + \rho_n^{core}(r)$ ).  $\rho_{n/p}^{halo}(r)$  in Eq. (1), represents the density distribution for halo part and it is calculated using transformed HO (THO) radial wavefunctions based on LST as follows [12]:

$$\rho_{n/p}^{halo}(r) = \frac{1}{4\pi} X_{n/p}^{nlj,halo} |R_{nl}^{THO}(r, b_{n/p})|^2 \quad (3)$$

where

$$R_{nl}^{THO}(r, b_{n/p}) = \frac{f(r)}{r} \sqrt{\frac{df(r)}{dr}} R_{nl}(f(r), b_{n/p}) \quad (4)$$

and

$$f(r) = \left[ \frac{1}{\left(\frac{1}{r}\right)^m + \left(\frac{1}{\gamma\sqrt{r}}\right)^m} \right]^{\frac{1}{m}} \quad (5)$$

$X_{n/p}^{nlj,halo}$  in Eq. (3), represents the occupation numbers of neutron(s)/proton(s) in the halo part.  $f(r)$  in Eq. (4), represents a function chosen so as to reproduce the proper asymptotic condition (exponential shape) for the density distribution at large  $r$ , besides it leaves the interior shape of density unchanged [12].  $m$  and  $\gamma$  in Eq. (5) are an integer and real numbers controls how sharply the tail of wave function will be; such technique is going to be called HO+LST.

Again, the matter density distribution for whole halo nucleons can be written as a sum the densities of halo neutrons and protons ( $\rho_m^h(r) = \rho_p^h(r) + \rho_n^h(r)$ ).

The charge density distribution (CDD),  $\rho_{ch}(r)$  of the nucleus is obtained by folding the point proton density in Eq. (1) with the charge density distribution of the proton itself as follows [18]:

$$\rho_{ch}(r) = \int \rho_p(r) \rho_{pr}(\mathbf{r} - \mathbf{r}') d\mathbf{r}' \quad (6)$$

where  $\rho_{pr}(\vec{r})$  is taken to have a Gaussian form [18]:

$$\rho_{pr}(r) = \frac{1}{(\sqrt{\pi}a_{pr})^3} e^{\left(\frac{-r^2}{a_{pr}^2}\right)} \quad (7)$$

where  $a_{pr} = 0.65 \text{ fm}$  is chosen such that to produce the experimental *rms* charge radius of the proton to be  $\langle r^2 \rangle_{pr}^{1/2} = \left(\frac{3}{2}\right)^{1/2} a_{pr} \approx 0.8 \text{ fm}$ .

Another way to reproduce the tail in the density is by using two HO size parameters, one for the compact core ( $b_{n/p}^c$ ) and the second for halo part ( $b_{n/p}^h$ ); such technique is going to be called HO+HO. The point neutron/proton density distribution in such away can be written as [16]:

$$\rho_{n/p}(r) = \rho_{n/p}^{core}(r, b_{n/p}^c) + \rho_{n/p}^{halo}(r, b_{n/p}^h) \quad (7)$$

The *rms* radii of neutron, proton, charge and matter can be directly calculated from their density distributions [18]:

$$\langle r^2 \rangle_X^{1/2} = \sqrt{\frac{4\pi}{X} \int_0^\infty \rho_X(r) r^2 dr} \quad (8)$$

In Eq. (8),  $X$  denotes to  $N$  (number of neutrons),  $Z$  (atomic number) and  $A$  (mass number), respectively.

In the first Born approximation, the longitudinal electron scattering form factors off nuclei can be written as [19, 20]:

$$|F_{J,ch}^C(q)|^2 = \frac{4\pi}{Z^2(2J_i+1)} |\langle J_f | \mathbf{O}_{J,t_z=1/2}^C(q) | J_i \rangle|^2 f_p^2(q) \quad (9)$$

where  $q$  and  $t_z$  represent the momentum transfer from electron to nucleus during scattering and isospin quantum number for nucleon ( $t_z = \frac{1}{2}$  for proton and  $t_z = -\frac{1}{2}$  for neutron).  $|J_i\rangle$  and  $|J_f\rangle$  are the initial and final states of the nucleus.  $f_p(q)$  is the charge form factor of a single proton given by Fourier transforms to Eq. (7).  $\mathbf{O}_{J,t_z=1/2}^C(q)$  represents the Coulomb multipole operator of the longitudinal electron scattering given by [19,20]:

$$\mathbf{O}_{J,t_z=1/2}^C(q) = e_{t_z=1/2} \sum_{i=1}^Z j_J(qr_i) Y_{JM_J}(\Omega_{r_i})$$

where  $j_J(qr_i)$  and  $Y_{JM_J}(\Omega_{r_i})$  are spherical Bessel and spherical harmonics functions, correspondingly.  $e_{t_z=1/2}$  is the charge of a single proton.

Eq. (9) can be simplified to be related to transition charge density distribution as following [19]:

$$|F_{J,ch}^C(q)|^2 = \frac{4\pi}{Z^2(2J_i+1)} \left| \int_0^\infty j_J(qr) \rho_{J,ch}(r) r^2 dr \right|^2 \quad (10)$$

where  $\rho_{J,ch}(r)$  is charge transition density distribution. For  $J = 0$ , Eq. (10) can be written as [19]:

$$|F_{J,ch}^C(q)|^2 = \left(\frac{4\pi}{qZ}\right)^2 \left| \int_0^\infty \sin(qr) \rho_{ch}(r) r dr \right|^2 \quad (11)$$

## Results and Discussion

The LST is used to improve the performance the radial wave functions of the HO potential. The exotic  ${}^{6,8}\text{He}$ ,  ${}^8\text{B}$ ,  ${}^{19}\text{C}$  and  ${}^{17}\text{Ne}$  nuclei are divided into two parts; the first is the stable core studied using the radial wave functions of HO potential, the second is the unstable exotic parts which is studied using the modified HO wavefunctions under LST technique. The MDDs, *rms* proton, charge, neutron, and matter radii, besides elastic electron scattering charge form factor are computed. Besides, two HO size parameters are used to regenerate aforementioned quantities; one for protons ( $b_p$ ) and the second for neutrons ( $b_n$ ).

The properties of the nuclei under study are presented in table 1. In Table- 2, the parameters,  $b_p$ ,  $b_n$ ,  $m$  and  $\gamma$  used to fulfill the calculations are tabulated. Such parameters are chosen so as to reproduce the *rms* radii and the tail in the density distribution.

The calculated proton, charge, neutron, and matter *rms* radii HO+LST technique are shown in table 3. In table 4, the same things that mentioned in table 3 are calculated and presented, but using the technique of HO+HO. Very good agreements are obtained for the calculated *rms* radii in comparison with the corresponding to the experimental data for all nuclei under study in both HO+LST and HO+HO techniques.

The calculated MDDs are depicted in Figures- 1(a, b, c ,d and e) for  ${}^6\text{He}$ ,  ${}^8\text{He}$ ,  ${}^8\text{B}$ ,  ${}^{19}\text{C}$  and  ${}^{17}\text{Ne}$  nuclei, respectively. The solid and dashed curves represent the calculated matter density distributions in HO+LST and HO+HO respectively. In general, it is clear that there are good agreements for the calculated MDDs with experimental data in HO+LST technique, where the long tail behavior which is a distinguishing feature of halo nuclei is well generated for the calculated matter density distribution.

In Figs. 2(a), (b), (c), (d) and (e), the elastic electron scattering form factors in plane wave Born approximation for  ${}^6\text{He}$ ,  ${}^8\text{He}$ ,  ${}^8\text{B}$ ,  ${}^{19}\text{C}$  and  ${}^{17}\text{Ne}$  nuclei are presented by solid and dashed curves for HO+LST and HO+HO techniques, respectively. The calculated charge form factors in HO+HO for all nuclei shift downwards on contrary to the calculated results of HO+LST which enhance form factors and shift the results upwards. The calculated charge form factors for the aforementioned nuclei are future predictions for the planned electron colliders which may provide us with experimental data.

**Table 1-** Properties of exotic  ${}^6\text{He}$ ,  ${}^8\text{He}$ ,  ${}^8\text{B}$ ,  ${}^{19}\text{C}$  and  ${}^{17}\text{Ne}$  nuclei

${}^A_Z X_N$	$J^\pi$ [21]	Half-Life Time [21]	Type	Separation Energies
${}^6_2 \text{He}_4$	$0^+$	$t_{1/2} = 806.92 \text{ ms}$	2n Halo [22]	$S_{2n} = 0.97$ [23]
${}^8_2 \text{He}_6$	$0^+$	$t_{1/2} = 119.1 \text{ ms}$	4n Skin [22]	$S_{2n} = 2.13$ [23] $S_{4n} = 3.10$
${}^8_5 \text{B}_3$	$2^+$	$t_{1/2} = 770 \text{ ms}$	1p Halo [22]	$S_p = 0.138$ [23]
${}^{19}_6 \text{C}_{13}$	$1/2^+$	$t_{1/2} = 46.2 \text{ ms}$	1n Halo [22]	$S_n = 0.53$ [23]
${}^{17}_{10} \text{Ne}_7$	$1/2^-$	$t_{1/2} = 109.2 \text{ ms}$	2p Halo [22]	$S_{2p} = 0.95$ [23]

**Table 2-**The HO size parameters and  $\gamma$  for exotic  ${}^6\text{He}$ ,  ${}^8\text{He}$ ,  ${}^8\text{B}$ ,  ${}^{19}\text{C}$  and  ${}^{17}\text{Ne}$  nuclei

${}^A_Z X_N$	$b_p(\text{fm})$	$b_n(\text{fm})$	Halo state	$m$	$\gamma(\text{fm}^{-1})$
${}^6_2 \text{He}_4$	1.559	1.547	$1p_{3/2}$	6	1.5
${}^8_2 \text{He}_6$	1.435	1.362	$1p_{3/2}$	4	1.435
${}^8_5 \text{B}_3$	1.6	1.595	$1p_{1/2}$	10	1.360
${}^{19}_6 \text{C}_{13}$	1.631	1.951	$2s_{1/2}$	16	1.693
${}^{17}_{10} \text{Ne}_7$	1.657	1.64	$1d_{5/2}$	8	1.617

**Table 3-** Calculated and experimental proton, charge, neutron, and matter *rms* radii in Fermi's for exotic  ${}^6\text{He}$ ,  ${}^8\text{He}$ ,  ${}^8\text{B}$ ,  ${}^{19}\text{C}$  and  ${}^{17}\text{Ne}$  nuclei using HO+LST technique

${}^A_Z X_N$	$\langle r^2 \rangle_p^{1/2}$	Exp. $\langle r^2 \rangle_p^{1/2}$	$\langle r^2 \rangle_{ch}^{1/2}$	Exp. $\langle r^2 \rangle_{ch}^{1/2}$	$\langle r^2 \rangle_n^{1/2}$	Exp. $\langle r^2 \rangle_n^{1/2}$	$\langle r^2 \rangle_m^{1/2}$	Exp. $\langle r^2 \rangle_m^{1/2}$
${}^6_2 \text{He}_4$	1.909	1.925(12) [22]	2.068	2.068(10) [22]	2.749	2.74(7) [22]	2.500	2.50(5) [22]
${}^8_2 \text{He}_6$	1.757	1.807(28) [22]	1.929	1.929(26) [22]	2.702	2.72(4) [22]	2.500	2.52(3) [22]
${}^8_5 \text{B}_3$	2.742	2.76(8) [24]	2.827	2.82(6) [25]	2.159	2.16(8) [24]	2.539	2.55(8) [24]
${}^{19}_6 \text{C}_{13}$	2.401	2.40(3) [26]	2.529	-	3.455	-	3.161	3.16(7) [26]
${}^{17}_{10} \text{Ne}_7$	2.948	-	3.041	3.042(21) [27]	2.440	-	2.750	2.75(7) [28]

**Table 4-** Calculated and experimental proton, charge, neutron, and matter *rms* radii in Fermi's for exotic  ${}^6\text{He}$ ,  ${}^8\text{He}$ ,  ${}^8\text{B}$ ,  ${}^{19}\text{C}$  and  ${}^{17}\text{Ne}$  nuclei using HO+HO technique

${}^A_Z X_N$	Core	halo	$\langle r^2 \rangle_p^{1/2}$	Exp. $\langle r^2 \rangle_p^{1/2}$	$\langle r^2 \rangle_{ch}^{1/2}$	Exp. $\langle r^2 \rangle_{ch}^{1/2}$	$\langle r^2 \rangle_n^{1/2}$	Exp. $\langle r^2 \rangle_n^{1/2}$	$\langle r^2 \rangle_m^{1/2}$	Exp. $\langle r^2 \rangle_m^{1/2}$
${}^6\text{He}$	$b_p^c = 1.559$ $b_n^c = 1.559$	$b_n^h = 2.141$	1.909	1.925(12) [22]	2.068	2.068(10) [22]	2.748	2.74(7) [22]	2.50	2.50(5) [22]
${}^8\text{He}$	$b_p^c = 1.435$ $b_n^c = 1.435$	$b_n^h = 1.961$	1.758	1.807(28) [22]	1.929	1.929(26) [22]	2.727	2.72(4) [22]	2.52	2.52(3) [22]
${}^8\text{B}$	$b_p^c = 1.6$ $b_n^c = 1.595$	$b_p^h = 2.617$	2.742	2.76(8) [24]	2.855	2.82(6) [25]	2.16	2.16(8) [24]	2.54	2.55(8) [24]
${}^{19}\text{C}$	$b_p^c = 1.631$ $b_n^c = 1.75$	$b_n^h = 3.391$	2.401	2.40(3) [26]	2.529	-	3.261	-	3.016	3.16(7) [26]
${}^{17}\text{N}_e$	$b_p^c = 1.61$ $b_n^c = 1.60$	$b_p^h = 2.38$	2.938	-	3.043	3.042(21) [27]	2.381	-	2.722	2.75(7) [28]

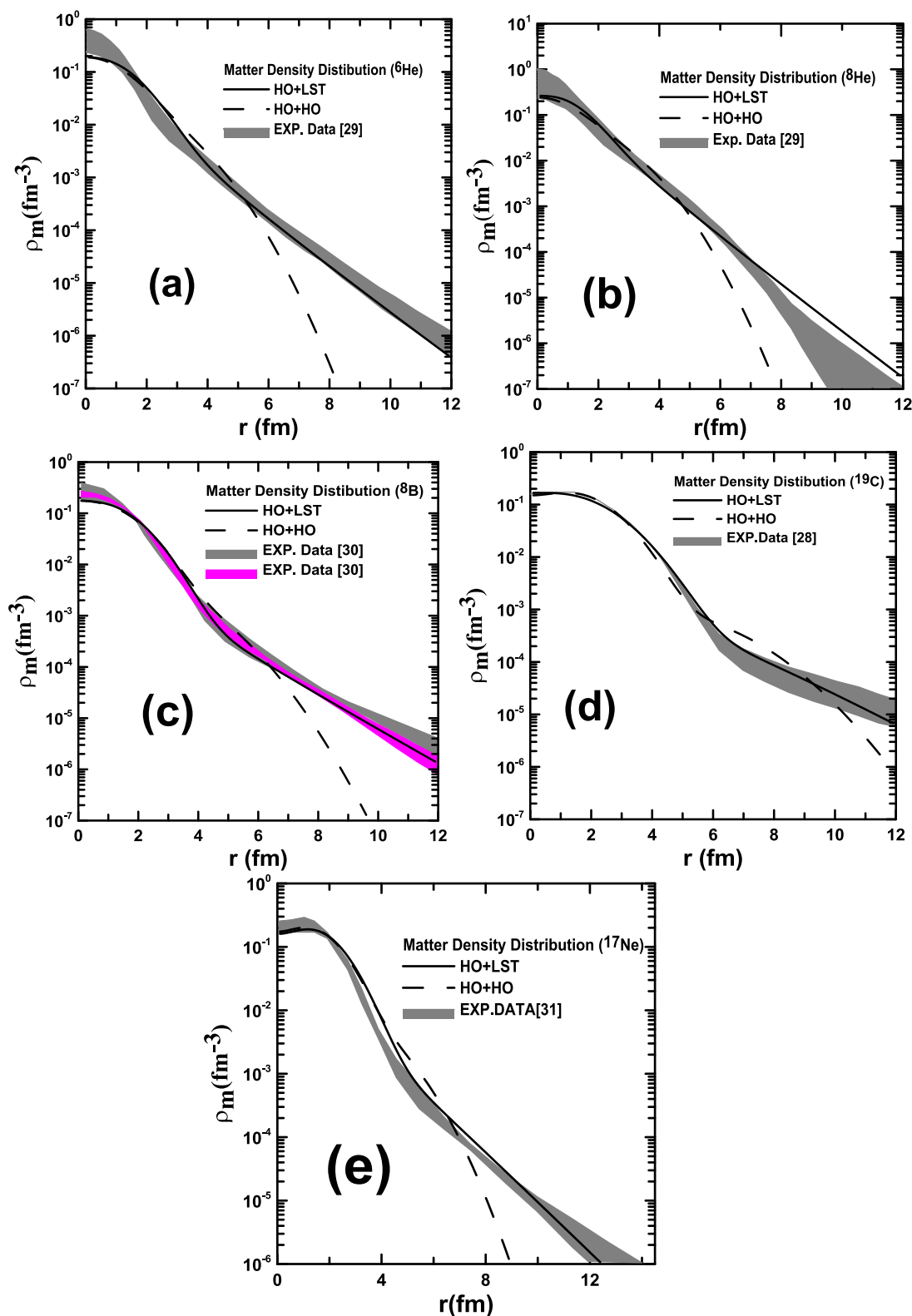


**Figure 1**-The calculated MDDs for exotic  ${}^6\text{He}$  (a),  ${}^8\text{He}$  (b),  ${}^8\text{B}$  (c),  ${}^{19}\text{C}$  (d) and  ${}^{17}\text{Ne}$  (e) nuclei represented by solid and dashed curves, respectively. The shaded areas are experimental data.

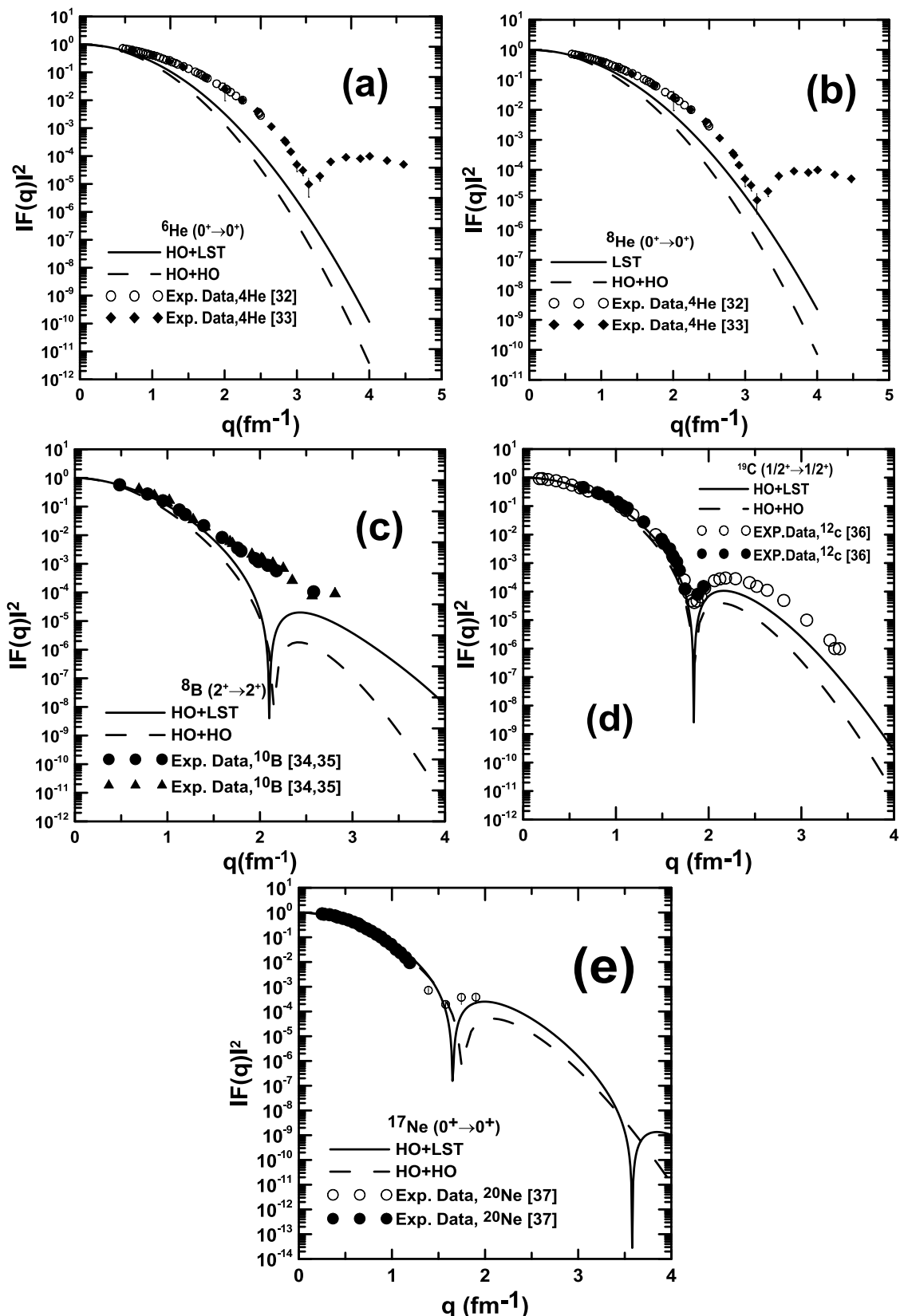


**Figure 2-** The calculated charge form factors for exotic  ${}^6\text{He}$  (a),  ${}^8\text{He}$  (b),  ${}^8\text{B}$  (c),  ${}^{19}\text{C}$  (d) and  ${}^{17}\text{Ne}$  (e) nuclei represented by solid and dashed curves, respectively.

### Conclusions

The LST is applied to the exotic nucleons for neutron-rich  ${}^{6,8}\text{He}$  and  ${}^{19}\text{C}$  nuclei and proton-rich  ${}^8\text{B}$  and  ${}^{17}\text{Ne}$  nuclei to find the nuclear proton, charge, neutron and matter root-mean square radii and corresponding density distributions and elastic electron scattering charge form factors. Such technique

unstable one to improve the HO radial wave functions successfully to reproduce the tail behavior in MDDS at high  $r$  which is the main characteristic of halo nuclei. Two approaches are used in this work, the first is HO+HO using two HO size parameters one for stable core and the second for unstable halo part. The second approach is HO+LST, where one HO size parameter is applied for the whole nuclear system, but LST is applied for exotic nucleons. Good agreement results are obtained for aforementioned quantities.

## References

1. Tanihata, I., Hamagaki, H., Hashimoto, O., Shida, Y., Yoshikawa, N., Sugimoto, K., Yamakawa, O., and Kobayashi, T. **1985**. Measurement of interaction cross sections and nuclear radii in the light p-shell region. *Physical Review Letters*, **55**(24): 2676-2679.
2. Hansen, P. G. and Jonson, B. **1987**. The neutron halo of extremely neutron-rich nuclei. *Europhysics Letters*, **4**(4): 409-414.
3. Navratil, P. and Barrett, B. R. **1996**. No-core shell-model calculations with starting-energy-independent multivalued effective interactions. *Physical Review C*, **54**(6): 2986-2995.
4. Caurier, E. and Navratil, P. **2006**. Proton radii of  $^{4,6,8}\text{He}$  isotopes from high-precision nucleon-nucleon interactions. *Physical Review C*, **73** (021302(R)): 1-5.
5. Karatagliidis, S., Amos, K., Fraser, P., Canton, L. and Svenne, J. P. **2008**. Constraints on the spectra of  $^{17,19}\text{C}$ . *Nuclear Physics A*, **813**: pp. 235-251.
6. Navratil, P. and Barrett, B. R. **1998**. Large- basis shell-model calculations for p-shell. *Physical Review C (Nuclear Physics)*, **57**(6): 3119-3128
7. Kuo, T. T. S., Muether, H. and Amir-Azimi-Nili, K. **1996**. Realistic effective interactions for halo nuclei. *Nuclear Physics A*, **606**: 15-26.
8. Kuo, T. T. S., Krmpotic, F. and Tzeng, Y. **1997**. Suppression of corepolarization in halo nuclei. *Physical Review Letters*, **78**(14): pp. 2708-2711.
9. Adel, K. H., Raad, A. R. and Arkan, R. R. **2012**. Theoretical study of matter density distribution and elastic electron scattering form factors for the neutron-rich  $^{22}\text{C}$  exotic nucleus. *Iraqi Journal of Physics*, **10** (19): pp. 25-34.
10. Stoitsov, M. V., Ring, P., Vretenar, D., and Lalazissis, G. A. **1998**. Solution of relativistic Hartree-Bogoliubov equations in configurational representation: Spherical neutron halo nuclei. *Physical Review C*, **58**(4): 2086- 2091.
11. Stoitsov, M. V., Nazarewicz, W., and Pittel, S. **1998**. New discrete basis for nuclear structure studies. *Physical Review C*, **58**(4): 2092- 2098.
12. Karatagliidis, S. and Amos, K. **2005**. Local scale transformations and extended matter distributions in nuclei. *Physical Review C*, **71** (064601): 1-13.
13. Lay, J. A., Moro, A. M., and Arias, J. M. **2010**. Exploring continuum structures with a pseudo-state basis. *Physical Review C*, **82** (024605): 1-11.
14. Stoitsov, M. V., Schunck, N., Kortelainen, M., Michel, N., Nam, H. Olsen, E., Sarich, J. and Wild S. **2013**. Axially deformed solution of the Skyrme-Hartree-Fock-Bogolyubov equations using the transformed harmonic oscillator basis (II) HFBTHO v2.00d: a new version of the program. *Computer Physics Communications*, **184**: 1592-1604
15. Navarro Perez, R., Schunck, N., Lasseri, R.-D., Zhang, C. and Sarich, J. **2017**. Axially deformed solution of the Skyrme-Hartree-Fock-Bogolyubov equations using the transformed harmonic oscillator basis (III) HFBTHO (v3.00): A new version of the program. *Computer Physics Communications*, **220**: 363-375.
16. Hamoudi, A. K., Radhi, R. A. and Ridha, A. R. **2015**. Elastic electron scattering from  $^{17}\text{Ne}$  and  $^{27}\text{P}$  exotic nuclei. *Iraqi Journal of Physics*, **13**: 68-81.
17. Brussard, A. P. J. and Glademans, P. W. M. **1977**. Shell-model Application in Nuclear Spectroscopy. North-Holland Publishing Company, Amsterdam.
18. Elton, L. R. B. and Swift, A. **1967**. Single-particle potentials and wave functions in the 1p and 2s-1d shells. *Nuclear Physics A*, **94**: 52-72.
19. Deforest, T. Jr. and Walecka, J. D. **1966**. Electron scattering and nuclear structure. *Advances in Physics*, **15**: 1-109.

20. Brown, B. A., Wildenthal, B. H., Williamson, C. F., Rad, F. N., Kowalski, S., Crannell, H., O'Brien, J. T. **1985**. Shell-model analysis of high-resolution data for elastic and inelastic electron scattering on  $^{19}\text{F}$ . *Physical Review C*, **32**: 1127-1145.
21. Audi, G., Kondev, F.G., Meng Wang, Huang, W.J., and Naimi, S. **2017**. The NUBASE2016 evaluation of nuclear properties. *Chinese Physics C*, **41** (030001): 1-138.
22. Tanihata, I., Savajols, H., and Kanungo, R. **2013**. Recent experimental progress in nuclear halo structure studies. *Progress in Particle and Nuclear Physics*, **68**: 215-313.
23. Jensen, A. S., Riisager, K., and Fedorov, D. V. **2004**. Structure and reactions of quantum halos . *Reviews of Modern Physics*, **76**: 215-261.
24. Chadel, S. S., Dhiman, S. K. and Shyam, R. **2003**. Structure of  $^8\text{B}$  and astrophysical  $S_{17}$  factor in Skyrme Hartree-Fock theory. *Phys. Rev. C*, **68**(054320): 1-19.
25. Blank, B., Marchand, C., Pravikoff, M.S., Baumann, T., Boué, F., Geissel, H., Hellström, M., Iwasab, N., Schwab, W., Sümmerer, K., and Gai, M. **1997**. *Nuclear Physics A*, **624**: 242-256.
26. Kanungo, R., Horiuchi, W., Hagen, G., Jansen, G. R., Navratil, P., Ameil, F., Atkinson, J., Ayyad, Y., Cortina-Gil, D., Dillmann, I., Estrade, A., Evdokimov, A., Farinon, F., Geissel, H., Guastalla, G., Janik, R., Kimura, M., Knobel, R., Kurcewicz, J., Yu. Litvinov, A., Marta, M., Mostazo, M., Mukha, I. , Nociforo, C., Ong, H.J. , Pietri, S., Prochazka, A., Scheidenberger, C., Sitar, B. , Strmen, P., Suzuki, Y., Takechi, M., Tanaka, J., Tanihata, I., Terashima, S., Vargas, J., Weick, H., and Winfield, J. S. **2016**. Proton Distribution Radii of  $^{12-19}\text{C}$  Illuminate Features of Neutron Halos. *Physical Review Letters*, **117** (102501): 1-5.
27. Geithner, W., Neff, T., Audi, G., Blaum, K., Delahaye, P., Feldmeier, H., George, S., Guénaut, C., Herfurth, F., Herlert, A., Kappertz, S., Keim, M., Kellerbauer, A., Kluge, H.-J., Kowalska, M., Lievens, P., Lunney, D., Marinova, K., Neugart, R., Schweikhard, L., Wilbert, S., and Yazidjian, C. **2008**. Masses and charge radii of  $^{17-22}\text{Ne}$  and the two-proton-halo candidate  $^{17}\text{Ne}$  .*Physical Review Letters*, **101** (252502): 1-4.
28. Ozawa A., Suzuki T., and Tanihata I. **2001**. Nuclear size and related topics. *Nuclear Physics A*, **693**: 32-62.
29. Takechi, M., Fukuda, M., Mihara, M., Matsumiya, R.; Matsuta, K.; Minamisono, T.; Ohtsubo, T.; Izumikawa, T.; Momota, S.; Suzuki, T.; Yamaguchi, T.; Nakajima, S.; Kobayashi, K.; Tanaka, K.; Suda, T.; Sato, S.; Kanazawa, M.; Kitagawa. **2007**. A. Precise Studies of Nucleon Density Distribution of  $^6\text{He}$  and  $^8\text{He}$ . *American Institute of Physics Conference Proceedings*, **891**: 187–191.
30. Takechi, M. M., Fukuda, M. Mihara, T. Chinda, T. Matsumasa, H. Matsubara, Y. Nakashima, K. Matsuta, T. Minamisono, R. Koyama, W. Shinosaki, M. Takahashi, A. Takizawa, T. Ohtsubo, T. Suzuki, T. Izumikawa, S. Momota, K. Tanaka, T. Suda, M. Sasaki, S. Sato, A. Kitagawa. **2005**. Reaction cross-sections for stable nuclei and nucleon density distribution of proton drip-line nucleus  $^8\text{B}$ . *The European Physical Journal A (Hadrons and Nuclei)*, **25** (s01): 217-219.
31. Tanaka, K. M. Fukuda, M. Mihara, M. Takechi, T. Chinda, T. Sumikama, S. Kudo, K. Matsuta, Zheng Tao. **2005**. Nucleon density distribution of proton-drip nucleus  $^{17}\text{Ne}$ . *The European Physical Journal A (Hadrons and Nuclei)*, **25** (s01): 221-222.
32. Frosch, R. F., McCarthy, J. S., Rand,R. E. and Yearian, M. R. **1968**. Structure of the  $\text{He}^4$  nucleus from elastic electron scattering. *Physical Review*, **160**: 874-879.
33. Arnold, R. G., Chertok, B. T., Rock, S., Schütz, W. P., Szalata, Z. M., Day, D. J., McCarthy, S., Martin, F., Mecking, B. A., Sick, I. and Tamas, G. **1978**. Elastic Electron Scattering from  $^3\text{He}$  and  $^4\text{He}$  at High Momentum Transfer. *Physical Review Letters*, **40**: 1429-1432.
34. Stovall, T., Goldemberg, J. and Isabelle, D. B. **1966**. Coulomb form factors of  $^{10}\text{B}$  and  $^{11}\text{B}$ . *Nuclear Physics A*, **86**: 225-240.
35. Cichocki, A., Dubach, J., Hicks, R. S., Peterson, G. A., De Jager, C. W., De Vries, H., Kalantar-Nayestanaki, N. and Sato, T. **1995**. Electron scattering from  $^{10}\text{B}$ . *Physical Review C*, **51**: 2406-2426.
36. Sick, I. and McCarthy, J. S. **1970**. Elastic electron scattering from  $^{12}\text{C}$  and  $^{16}\text{O}$ . *Nuclear Physics A*, **150**: 631-654.
37. E. A. Knight, R. P. Singhal, R. G. Arthur, and M. W. S. Macauley. **1981**. Elastic scattering of electrons from  $^{20,22}\text{Ne}$ . *Journal of Physics G (Nuclear Physics)*, **7**: 1115-1121.